

PCCP

Accepted Manuscript



This is an *Accepted Manuscript*, which has been through the Royal Society of Chemistry peer review process and has been accepted for publication.

Accepted Manuscripts are published online shortly after acceptance, before technical editing, formatting and proof reading. Using this free service, authors can make their results available to the community, in citable form, before we publish the edited article. We will replace this *Accepted Manuscript* with the edited and formatted *Advance Article* as soon as it is available.

You can find more information about *Accepted Manuscripts* in the [Information for Authors](#).

Please note that technical editing may introduce minor changes to the text and/or graphics, which may alter content. The journal's standard [Terms & Conditions](#) and the [Ethical guidelines](#) still apply. In no event shall the Royal Society of Chemistry be held responsible for any errors or omissions in this *Accepted Manuscript* or any consequences arising from the use of any information it contains.

Structure Formation in Diindenoperylene Thin Films on Copper(111)

H. Aldahhak, W. G. Schmidt, and E. Rauls

Lehrstuhl für Theoretische Physik, Universität Paderborn, 33095 Paderborn, Germany

S. Matencio, E. Barrena, and C. Ocal

Instituto de Ciencia de Materiales de Barcelona (ICMAB-CSIC), Campus de la UAB, 08193 Bellaterra, Spain

(Dated: February 6, 2015)

First-principles calculations were combined with scanning tunneling microscopy (STM) measurements to analyze the adsorption of diindenoperylene (DIP) molecules on Cu(111) surfaces. The influence of the substrate on the geometry of single adsorbed molecules, their diffusion barriers, as well as the role of step-edges and intermolecular interactions for molecular self-assembly and structure growth are studied. Long-range ordered arrangements of DIP molecules are found to be most favorable irrespective of the terrace width. Energetically less favored short-range order structures, however, are observed as well.

Keywords: Cu(111), DIP, self assembly, step edges, ab initio, STM, PES, long-range, short-range, configurational entropy.

Molecular self-assembly is both scientifically interesting as well as of technological relevance as a possible route to nanoscale devices. Molecular self-organization into supramolecular structures on various substrates is driven by the delicate balance between the molecule-surface and the molecule-molecule interactions. Understanding these interactions is crucial in order to steer the structure growth, which is in turn relevant to the performance of the realized devices¹⁻⁵. Diindenoperylene (DIP, C₃₂H₁₆) is a planar perylene-based molecule, cf. Fig. 1a. Its ambipolar behavior⁶, its high stability against oxidation and at elevated temperatures (up to 730 K)⁷ as well as its very good film forming properties on different substrates⁸⁻¹⁰ make it a promising candidate for organic optoelectronic devices¹¹⁻¹³. This molecule has recently been studied on SiO₂¹⁴⁻¹⁶, Cu(100)¹⁷, Cu(111)¹⁸⁻²¹, Ag(111)²² and different Au surfaces²³⁻²⁹. DIP molecules exhibit different crystallographic growth patterns on these surfaces. They stand upright on SiO₂ and rubrene¹⁰, while, in contrast, they lie flat on various Au, Ag and Cu surfaces¹⁷⁻²⁹. On Au(100), Au(110) and Au(111) surfaces, different islands shapes and aggregation forms have been found depending on the surface orientation²⁷. Even on the same surface, such as Ag(111) for example, the first monolayer of DIP molecules may show different superstructures (herringbone or brick-wall superstructures) depending on the deposition rate²². Recent STM investigations of DIP on Cu(111) by some of the present authors found the self-assembled structures to depend on the terrace width¹⁸: On wider terraces (≥ 15 nm), DIP molecules adsorb in a short range order (SR) in which the molecules are arranged in domains oriented along the three equivalent crystal directions determined by the substrate symmetry (Fig. 1b). On narrower terraces (≤ 15 nm), molecules adopt a well-defined long-range adsorption order (LR) (Fig. 1c)¹⁸ with adjacent molecules oriented co-directionally in oblique cells described by $a=8.7\pm 0.4$ Å, $b=18.5\pm 0.7$ Å, $\gamma=71\pm 1^\circ$ (Fig. 1c). The present total-energy calculations find the long-range or-

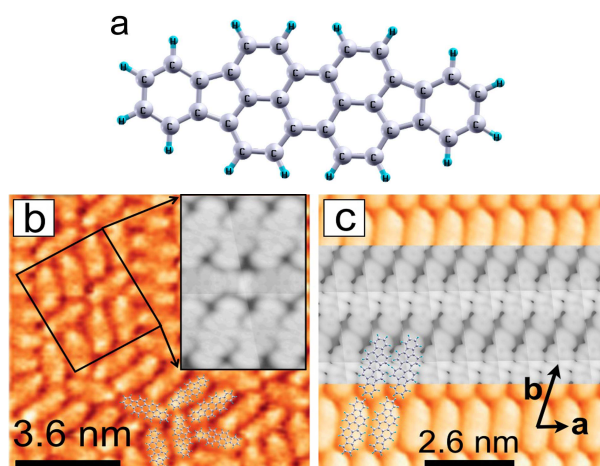


FIG. 1: (a) Ball-and-stick model of the DIP molecule. (b) The short-range (SR) and (c) the long-range (LR) arrangements of DIP molecules on Cu(111) terraces of different widths as observed experimentally using STM (cf. Ref. 18). Shown in gray are simulated STM images that were obtained using the Tersoff-Hamann model (cf. Ref. 30). Ball-and-stick models of DIP molecules illustrate the molecular positions on the substrate.

dered arrangements to be most favorable, irrespective of the terrace width. They indicate step-edges to trigger structure formation while thermal effects facilitate the appearance of less-ordered structures. The STM observations presented here demonstrate the co-existence of long- and short-range ordered domains no matter what the terrace width is.

The work is organized as follows: After a short methodological part, we first discuss the single molecule adsorption and then DIP monolayer configurations on the planar Cu(111) surface. Afterwards the role of step edges for molecular adsorption and structure-formation is investigated before we conclude.

I. METHODOLOGY

The adsorbate structures have been calculated using the Vienna Ab Initio Simulation Package (VASP) implementation³¹ of DFT. The Perdew-Wang 1991 functional (PW91)³² is used to model the electron exchange and correlation interaction within the generalized gradient approximation (GGA). The electron-ion interaction is described by the projector-augmented wave (PAW) method³³. Plane waves up to an energy cutoff of 340 eV are used as basis functions. We complemented the DFT total energy by an additional London-type correction³⁴ in order to account for dispersive forces numerically. This so-called DFT-D approach has been shown to yield remarkably reliable results for a variety of adsorbate systems, see, e.g. Refs. 35–38. The sampling of the Brillouin zone was done using a $(2 \times 2 \times 1)$ k-point grid. In all calculations, convergence criteria of 10^{-5} eV for the total energy and a convergence criterion of 0.03 eV/Å for the maximum final force were used. The repeated-slab method with a vacuum layer of 30 Å was used to simulate the surfaces. Detailed convergence tests³⁹ for various material slab thicknesses demonstrated that the use of six atomic Cu(111) layers is required for reliable adsorption energies and molecular geometries. This parameter has been used here. Thereby the atoms in the two lowest layers were kept frozen at ideal bulk positions during structure optimization. If not stated otherwise, the remaining substrate atoms as well as the adsorbate were allowed to relax freely. The same setup was used to model the step edges in a saw tooth-like model system, described in Ref. 40, with terraces wide enough to suppress interaction between periodic images of the molecule or the step itself. Adsorption energies (E_{ads}) have been calculated as $E_{ads} = E_{sys} - E_{sur} - E_{mol}$, where E_{sys} is the energy of the adsystem, while E_{sur} and E_{mol} are the energies of the substrate and the energy of the molecule in gas phase, respectively. A simple model where the DIP molecules are represented by parallelograms, which form various molecular superstructures, has been used to approximate the influence of the configurational entropy on the surface stability.

Measurements were carried out at room temperature using a commercial STM/nc-AFM (Specs GmbH) in ultra high vacuum (UHV), base pressure $\sim 5 \times 10^{-10}$ mbar. A KolibriSensor was used to perform simultaneous STM and non-contact AFM in the frequency modulation mode. The metallic tip, with resonant frequency $f_0 \approx 1$ MHz, was operated at an oscillation amplitude $A = 200$ pm after being in-situ cleaned by Ar⁺ sputtering. The Cu(111) single crystal (Matek GmbH, Germany), was prepared with repeated cycles of Ar⁺ sputtering plus annealing at 240° C. Diindenoperylene was evaporated from a Knudsen cell at 225° C at an evaporation rate of 0,05ML/min.

II. DIP MOLECULES ON PLANAR CU(111) SURFACES

Using normal-incidence x-ray standing wave (XSW) measurements, Bürker et al.²⁰ have reported the vertical distance of DIP molecules adsorbed on a Cu(111) surface to be 2.51 ± 0.03 Å. In those measurements, which were done for coverages between 0.3 and 0.9 ML, they found that the vertical DIP position weakly depends on the surface coverage. They confirmed their experimental results by DFT calculations²⁰. In agreement with that study, Schuler et al.²¹ have reported, using non-contact atomic force microscopy, that the geometry of the single DIP molecule slightly deviates from the planar adsorption form (see Ref. 20 and the supplemental materials of Ref. 21). In both studies, the orientation and the registry of the molecule were not determined.

A. Single-molecule adsorption

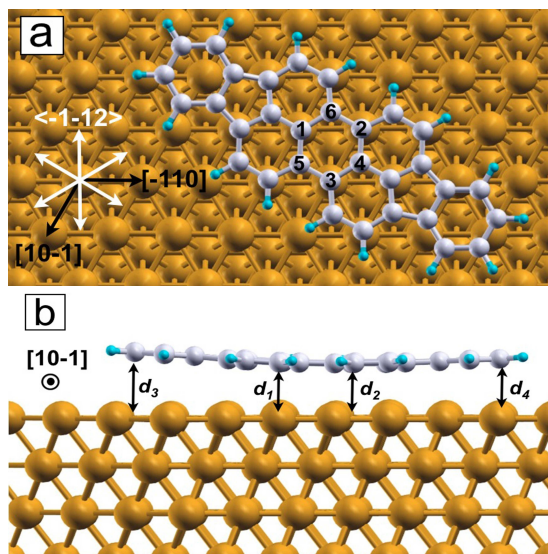


FIG. 2: (a) Top view and (b) side view of the most favored structure of single DIP molecules on Cu(111). The inner six carbon atoms are labelled from 1 to 6. The adsorption geometry is slightly concave. d_1 and d_2 denote the distances between carbon atom 1 and 2, respectively, to the Cu atoms beneath. Similarly, d_3 and d_4 denote the distances between the carbon atoms at both edges of the molecule and the Cu atoms beneath. Calculated values are given in Tab. I.

Supercells with (9×8) surface unit cells have been used for the single molecule calculations. In such supercells, we probed a large number of various adsorption sites including top, bridge, hcp- and fcc-hollow registries with different orientations of the molecule with respect to the surface, taking the center of the molecule as a refer-

	d_1	d_2	d_3	d_4
distance [Å]	2.54	2.48	2.93	2.63

TABLE I: Vertical distances between molecular atoms and the Cu(111) surface as defined in Fig. 2.

ence. In the most stable adsorption geometry, single DIP molecules adsorb parallel to the surface, although not completely flat. The long axis (LA) is parallel to one of the three equivalent $\langle 121 \rangle$ orientations of Cu(111). The molecule center is located over a hollow site with three out of the six inner carbon atoms (labelled 1 to 6 in Fig. 2a) residing on top of Cu atoms. Defining the height of the molecular center as the average between d_1 and d_2 (cf. Fig. 2b), the calculated distance between the center of the molecule and the surface (see Tab. I) fits perfectly to the experimental value of 2.51 \AA^{20} . It is also in good agreement with the calculated value by Bürker et al. (2.59 \AA^{20}). The small deviation with respect to Ref. 20 might be due to the thinner slab (3 layers compared to 6 layers in this work) they used to model the Cu(111) surface. Both sides of the molecule are lifted upwards by 0.12 \AA and 0.4 \AA with respect to its center (see Fig. 2b) resulting in a slightly concave and asymmetric adsorption geometry. This results confirms the experimental observations of a small molecular torsion (cf. Ref. 20 and 21). The adsorption energy of this structure is -4.84 eV which agrees well with the results obtained by Bürker et al.²⁰ (-4.74 eV). The rather high adsorption energies imply a strong molecule–substrate interaction.

In order to assess the mobility of the molecule on the surface, we determined the diffusion barriers of the molecule by calculating the potential energy surfaces (PESs) of the molecule on the surface for two cases (Fig. 3): in the first case, the molecule was moved laterally with its LA kept parallel to the $[1\bar{1}2]$ (Fig. 3a). In the second case, it was kept parallel to the $[1\bar{1}0]$ direction of the surface (Fig. 3b). The adsorption energies are laterally sampled on a dense mesh with a distance of 0.1 \AA between the grid points throughout the surface unit cell. The center of the molecule is taken as a reference. Thereby, the lateral position of carbon atom 1 direction (Fig. 2) was fixed, whereas all other degrees of freedom were structurally relaxed. In spite of the strong molecule–surface interactions, the calculated PESs show only a small corrugation of 0.35 eV . Accordingly, the DIP molecules are highly mobile already at low temperatures, thus enabling efficient molecular assembling. For the most unfavorable structure, the center of the molecule resides on a bridge site, while its LA is parallel to the $[1\bar{1}0]$ direction (denoted as B on Fig. 3b). The adsorption energy of this structure is -4.49 eV . While the top position is unfavorable when the LA is parallel to the $[1\bar{1}2]$ direction of the surface (-4.51 eV), it is more favorable (-4.72 eV) when the LA is parallel to the $[1\bar{1}0]$ direction. Accordingly, some favorable diffusion paths (e.g. from hollow to top positions) involve molecular rotations.

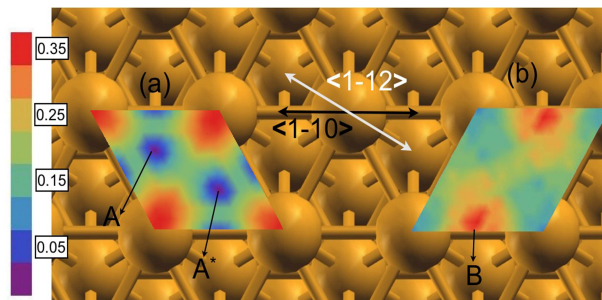


FIG. 3: The calculated PESs for single DIP molecules on Cu(111). The molecule was moved laterally and the LA was kept parallel to the (a) $[1\bar{1}2]$ and (b) $[1\bar{1}0]$ direction of the surface. The energetically most favoured structure is considered as the zero point on the scale (in eV). The most favorable hollow site A with the equivalent A^* sites are shown.

B. Molecular monolayers

The influence of the intermolecular interactions has been tested by calculating the adsorption energies of DIP molecules in different supramolecular arrangements. Beginning with commensurable structures, where the registry of the molecule corresponds to the most favorable single-molecule adsorption geometry, we obtained for the (9×6) , (9×4) , (7×8) , (7×6) and (7×4) supercells, energies of -4.82 eV , -5.55 eV , -5.05 eV , -4.91 eV and -5.49 eV , respectively. In most cases, molecule–molecule interactions increase the adsorption energy and, thus, stabilize the molecular aggregates. However, even more favorable structures can be found if we allow for denser arrangements of the molecules during aggregation. Like this, we can obtain structures which are closer to the ones that are experimentally observed¹⁸. We calculated a variety of possible cells considering different registries and orientations of the molecule on the surface. The highest adsorption energies were obtained for two oblique cells A and B, both defined by $A_1=B_1 = 8.77 \text{ \AA}$, $A_2=B_2 = 16.82 \text{ \AA}$, $\beta = 97.77^\circ$ (black arrows in Fig. 4a, b for A and B, respectively). The adstructures are arranged in a $\begin{pmatrix} A_1(B_1) \\ A_2(B_2) \end{pmatrix} = \begin{pmatrix} 4 & 2 \\ -1 & 6 \end{pmatrix} \begin{pmatrix} x_1 \\ x_2 \end{pmatrix}$ translational symmetry as depicted in (Fig. 4b). Here, x_1 and x_2 indicate the primitive vectors of Cu(111). These side-by-side molecular structures have the arrangement of the reported LR order (cf. Ref. 18) with unit cell dimensions very close to the measured values, i.e. $a = 8.77 \text{ \AA}$, $b = 17.89 \text{ \AA}$, $\theta = 69.68^\circ$ (white arrows depicted on Fig. 4a following the notation used by Oteyza et al.). For both structures, the registry of each molecule is almost similar to that of the single molecule, while the LA deviates by 10° from the $[1\bar{1}2]$ direction of the surface in order to avoid the repulsion between the hydrogen atoms of neighboring molecules (Fig. 4). This causes adjacent molecules to have their centers shifted along the LA with respect to each other. Phase A and

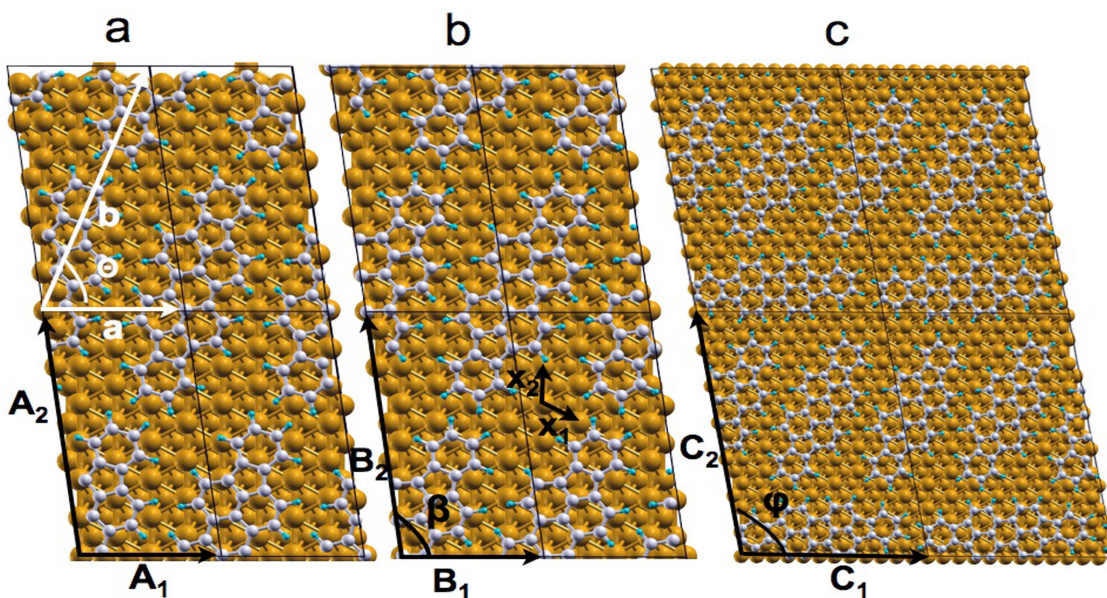


FIG. 4: Models of the two most stable phases found for the LR arrangement: phase A (a) and phase B (b) compared to the SR order (c).

phase B have the same dimensions, but differ in the orientation of the molecules within the unit cell. The adsorption energy/molecule for phase A is -5.63 eV, while it is -5.76 eV for phase B. We calculated the molecule-surface and the molecule-molecule contributions in the adsorption energies (Tab. II). Obviously, the molecule-molecule interactions gain importance in these structures, while the molecule-surface interactions are reduced compared to the single molecule adsorption. Correspondingly, the vertical molecule-surface distance is enlarged slightly to 2.90 Å and the molecule assumes an almost planar geometry. The finding that the vertical distance depends slightly on the molecular coverage is in agreement with experiment²⁰. We mention that DIP monolayers show a long-range arrangement on Cu(100) and Au(111) surfaces, with lattice parameters of $a = 10.5$ Å, $b = 18.6$ Å, $\theta = 92^\circ$ and dimensions of $a = 13.4$ Å, $b = 14.8$ Å, $\theta = 97^\circ$ on Cu(100)¹⁷ and Au(111)²⁶, respectively. For the SR order, we calculated a model comprising three molecules per unit cell. Two of them are arranged side-by-side with their long-axes parallel to each other while the third is rotated by 60° with respect to them. The individual molecules in the primitive unit cells have almost the registries of the molecules in the LR order, while their LAs are along two of the three equivalent $\langle 121 \rangle$ orientations of the surface (Fig.4c). The primitive unit cell is highlighted in Fig. 4c with the following parameters: $C_1 = 17.61$ Å, $C_2 = 25.83$ Å, $\varphi = 99.96^\circ$. The molecular density for the SR arrangement (σ_{SR}) is 0.66 molecules/ nm^2 . This fits perfectly with the value reported by Oteyza et al.¹⁸. The short-range order is slightly less dense than the LR order (σ_{LR}

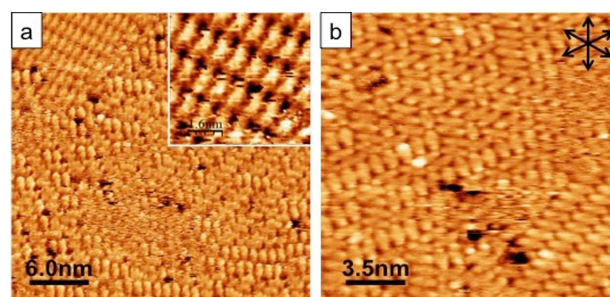


FIG. 5: STM images of DIP on Cu(111) for a submonolayer coverage, showing coexistence of LR ordered domains, SR order and a two-dimensional gas of mobile disordered molecules. (a) $I=370$ pA, bias= -0.37 V and (b) $I=130$ pA, bias= -1.25 V. The $\langle 110 \rangle$ substrate directions are indicated by black arrows, while gray arrows indicate the lattice vectors of the LR ordered domains.

$= 0.68$ molecules/ nm^2). The adsorption energy per molecule in this structure is -5.47 eV (molecule-surface contribution: -4.48 eV, molecule-molecule contribution -0.99 eV (Tab. II). The SR phase is energetically, thus, slightly less stable than the most stable LR orders. Our calculations thus predict that a monolayer of DIP on Cu(111) should show long-range domains on large terraces, or at least long-range order islands should be formed in co-existence with the short-range orders.

This fact has been confirmed by the STM experiments for a submonolayer coverage of molecules. Several structures with LR order have been observed in co-

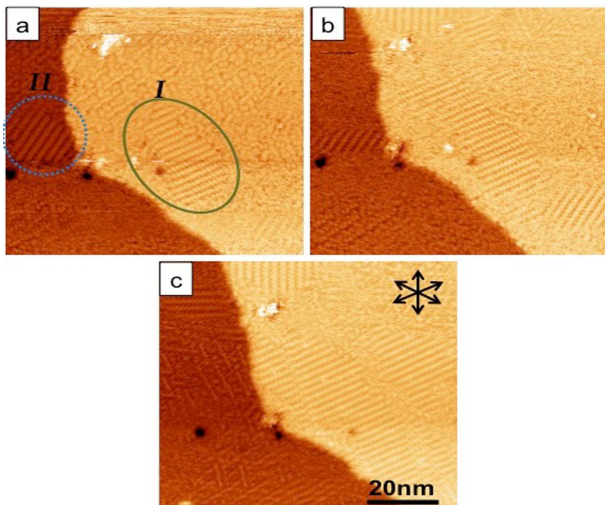


FIG. 6: (a)-(c) STM images acquired by continuous scanning in the same area ($I=90\text{pA}$, $\text{bias}=-0.45\text{V}$). (a) The LR ordered domain I is circled with a green continuous line, while domain II is circled with dotted blue line (see text for details). (b), (c) Consecutive tip scanning causes an increase of long-ranged ordering of I -type domains and the disappearance of the domain II .

existence with SR order and a two-dimensional gas of mobile molecules. The LR domains observed in Fig. 5a (top left) and Fig. 6 (domain I) agree reasonably well with the predicted structures A and B shown in the Fig. 4 ($A_1=9.1\text{ \AA}$, $A_2=16.3\text{ \AA}$, $\beta=100^\circ$). In addition, other domains with slightly different packing and orientation (Fig. 5b, Fig. 6a and b) are also observed. Notice in Fig. 5a the different alignment of the DIP molecules in single rows with their long axis oriented along the compact directions of the surface, i.e. $\langle 110 \rangle$ directions. The STM data shown in Fig. 6 demonstrate the formation of a LR ordered domain far from the step edge (domain I) which in this case appears surrounded by a region with SR order and mobile molecules. At the step edge of the lower terrace another ordered area is observed (domain II), which is 30° rotated with respect to domain I and has therefore the long axis of DIP aligned along one of the $\langle 110 \rangle$ directions. Consecutive scanning in the same area shows tip-induced reordering with two main effects: i) Increased area of domain I and growth of other domains equally oriented at expenses of regions with mobile molecules ii) Reduction and disappearance of the domain II giving rise to SR order. Although for these growth conditions, domains with DIP aligned along the $\langle 110 \rangle$ directions are formed, we conclude from the measurements that such an orientation is just metastable in agreement with the calculations.

structure	phase A	phase B	short-range
E_{ads} [eV]	-5.63	-5.76	-5.47
mol.-surf. contribution [eV]	-4.47	-4.50	-4.48
mol.-mol. contribution [eV]	-1.16	-1.26	-0.99

TABLE II: Comparison of the adsorption energies in the two most stable LR phases and the SR order.

III. DIP MOLECULES AT STEP EDGES

In the submonolayer DIP/Au(111) adsorption study, Oteyza et al.²⁶ reported step edges to initiate and steer the molecular assembly. DIP molecules are ordered in rows of head-to-tail configurations with the molecular long axes parallel to the step edge and following its azimuthal direction. In contrast, single DIP molecules on the more reactive Ag(111) surface²² decorate step-edges randomly. There, DIP molecules adsorb either parallel to the surface, with their molecular long axes parallel to the step-edge orientation, or tilted or bridging between the upper and the lower terrace. On these two surfaces as well as on Cu(100)¹⁷, step edges have been reported as preferred nucleation sites. On Cu(100), large ordered 2D islands of side-by-side DIP rows have been found to grow from the step edges, while smaller 2D islands on the terrace sites are formed¹⁷. However, in contrast to the stepped Au(111) surface²⁶, on the stepped Cu(100) surface, the molecular orientation is determined by the substrate, not the step direction.¹⁷.

A. Single molecules at Cu(111) step edges

In order to describe the behavior of single DIP molecules in the vicinity of the Cu(111) steps, monoatomic step edges along the $[1\bar{1}0]$ direction of the surface are modelled. A variety of structures, including different possible orientations and registries of the single DIP molecules with respect to the lower and upper terraces, have been tested (see Fig. 7). Beside the influence of the active step edge sites, single DIP molecules are subject to strong molecule-surface interactions. They show a variety of local probable structures with different orientations and registries with respect to the planar surface and to the step edge. For structures like A1, B4, C3, D6 and E0, adsorption energies of -5.36 eV, -5.27 eV, -5.47 eV, -5.99 eV and -6.17 eV, respectively, have been calculated (Fig. 7). In these structures, the molecules interact with the step edge with their main body residing on the lower terrace, while the outer carbon atoms bind to the upper terrace (see e.g. structures D6 and E0 in Fig. 8). Like this, step-edges are preferential adsorption sites for the mobile molecules, where these can finally be immobilized. This result, which is in agreement with similar systems^{17,22,26}, indicates that step edges serve as nucleation sites for structure formation. The influence of copper step edges on single DIP molecules is

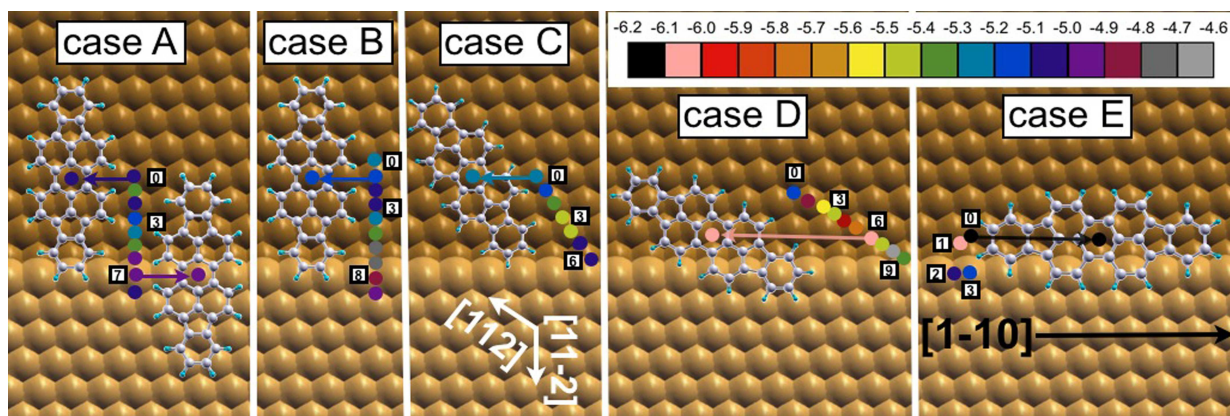


FIG. 7: Calculated adsorption geometries of DIP molecules at step edges. In case A and B, the molecular long axis (LA) is perpendicular to the step edge and parallel to the $[1\bar{1}2]$ direction of the lower surface. The molecule binds to one atom (two atoms) of the step edge in case A (case B). In case C (case D), the LA is tilted with respect to the step edge and it is oriented along the high symmetry $[\bar{1}01]$ ($[112]$) direction of the surface. In case E, the LA is parallel to the step-edge direction. For each case, a variety of registries with respect to the lower terrace have been tested. The center of the molecule is used as reference. The energies of the different structures are denoted as colored circles according to the energy scale on the upper panel. The atomic vdW-radius has been used for the Cu atoms. The upper terraces atoms have slightly lighter colors and some examples of the structures such as (A0, A7, B1, C0, D6 and E0) have been depicted in detail.

similar to Ag(111) surfaces but in contrast to Au(111) surfaces. This is plausible given the more reactive Ag and Cu surfaces compared to the Au(111) surface, which shows only weak molecule-surface interactions with the DIP aggregates²⁶. In contrast to Ag(111), DIP molecules on Cu(111) avoid bridging between the upper and lower terraces in agreement with the experiment¹⁸. Structures like A7, B7, C5, D8 and E2, which are direct examples of these cases, have adsorption energies of -4.95 eV, -4.69 eV, -5.02 eV, -4.6 eV and -5 eV, respectively. Thereby, they are locally less probable compared the previously mentioned structures (A1, B4, C3, D6 and E0). Molecules which extend on both the lower and the upper terrace suffer from strongly distorted geometries. This distortion manifests itself in deformation energies⁴¹ of +0.37 eV, +0.42 eV, +0.33 eV, +1.37 eV and +1.15 eV for A7, B7, C5, D8 and E2, respectively, which destabilize the corresponding structures. Two pronounced stable structures are D6 (Fig. 8a) and E0 (Fig. 8b) with adsorption energies of -5.99 eV and -6.17 eV, respectively. In both of them, the center of the molecule resides on the hollow surface position on the lower terrace. The LA forms an angle of 20° with the step-edge orientation in D6, while it is completely parallel to it in E0. The major parts of molecules reside on the lower surface, while the outer atoms bind to the step edge.

B. Molecular rows next to a step edge

Upon further deposition, i.e. at higher coverage, diffused molecules occupy the preferred nucleation step edges completely. The molecules, then, form a row close to the step edge. In this case, beside the influence of the step

edge and the substrate, the molecule-molecule interactions play a crucial role to steer and reorganize adjacent molecules. This forces the single molecules to arrange into an organized domain.

In order to quantify this effect, we calculated the adsorption energies for a variety of commensurable and incommensurable structures, beginning with the stable structures (A1, B4, C3, D6 and E0). The size of each aforementioned supercell has been reduced, in order to increase the molecule-molecule interactions, until we got the lowest adsorption energy. For the cases of incommensurable structures, we included two molecules in the unit cell.

The most stable structure of one row of DIP molecules is depicted in Fig. 8c. In this structure, the adsorption geometries of the two molecules contained in the unit cell are slightly different and denoted as α and β , respectively. The orientation and the registries of both α and β molecules resemble that of D6. With respect to the step-edge direction, the α (β) molecule is rotated by 22° (20°), the center of each molecule is still on a hollow site of the surface. The adsorption energy per molecule in this structure is -6.26 eV. The distance between the center of the α and β molecules is 16.47 Å, which is very close to that of the long-range arrangement on the planar surface. We note that the behavior of the first row of DIP molecules at Cu(111) step edges resembles that at the step edges of the Cu(100) surface, where DIP molecules are tilted with respect to step edges forming side-by-side rows¹⁷, but is in contrast to Au(111) step edges, where DIP molecules adsorb at the step edges in rows in a head-to-tail configuration with their long molecular axis aligned parallel to the step direction²⁶.

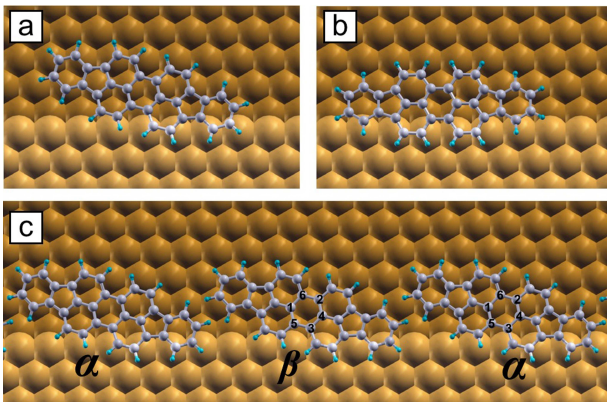


FIG. 8: Ball-and-stick representation of single DIP molecules at the Cu(111) step edges in the so-called (a) D6 and (b) E0 structures. (c) One row of molecules is shown. The molecules are arranged in incommensurable structures, where each one contains α and β molecules.

IV. DISCUSSION

While the present total-energy calculations show that the SR arrangement is less favorable than the LR order by about 0.3 eV per molecule, the two phases obviously co-exist as shown by STM. The appearance of different phases at the same time is likely to be related to the subtle balance between molecule-surface and the molecule-molecule interactions in both the LR and the SR order phase, cf. Tab. II. The molecule-surface interactions for the SR and the LR orders are almost the same (Tab. II). One expects that when the molecules are less densely packed on the surface they are mainly subject to the rather strong influence of the comparatively reactive Cu(111) surface, which determines the azimuthal molecular orientation and gives rise to three discrete equivalent orientations of the molecules on the surface which is a direct representation of the SR order. A transition from the SR order to an LR order then requires a collective rearrangement of the molecules that is kinetically hindered at room temperature. However, the existence of a coherent nucleation sites, e.g., straight step-edges, in combination with more gentle thermodynamic circumstances (i.e. higher substrate temperature and lower deposition rate) might help the molecules to be arranged in the LR order. Consequently adsorbed molecules will, at sufficiently low deposition rate, condense at the already existing LR domain and lead to an overall LR order.

One should state that the considerations so far do not take temperature effects into account⁴². Vibrational and configurational entropy contributions to the adlayer free energy will additionally modify the energetics at finite temperatures. A simple estimate for the configurational entropy difference between the LR and SR ordered

phase yields at 300K a free energy gain of about 0.1 eV/molecule for the latter. Also the slightly lower molecular density of the latter phase is expected to result in overall lower vibrational frequencies, which will for finite temperatures stabilize the SR order.

Which procedures can be thought of to assist in the formation of the LR ordered DIP structures on Cu(111)? One possibility is to increase the molecule-molecule interactions, so that they gain importance compared to the strong molecule-surface interactions. This could, e.g., be a complementary functional group or an adatom, like e.g. a mobile Cu atom. Such a partly catalytic and structure-controlling effect of metal atoms has e.g. been described in Ref. 43. Breaking the three-fold symmetry of the Cu(111) surface may also assist in LR ordering. This can be realized, e.g., by using a strained Cu(111) substrates. The first method has been applied by introducing copper-phthalocyanines (CuPc) or fluorinated copperphthalocyanines (F16CuPc)²³ with DIP molecules. The influence of lattice strain on the adsorption of molecules on a surface has, e.g., been investigated for PTCDA molecules on ionic substrates⁴⁴. A uniform strain was found to influence both the adsorption energies and the mobility of the molecules, such that the formation of phases which require a stronger reordering might be either promoted or hindered according to the strain parameter.

V. SUMMARY

In summary, we performed DFT calculations, supported by STM measurements, on the adsorption of DIP on Cu(111). Our results show an increase of the adsorption energy by going from isolated molecules to short-range and long-range ordered structures. The calculated adsorption geometries are in very good agreement with the experimental data available. The relatively low diffusion barriers calculated here in conjunction with the energetic most favorable adsorption at step edges suggest that the ordering of the molecular films may be initiated by straight steps and extends from there over the terraces. In addition to the most favorable structure, according to the calculations, experimentally other structures with different packing are found. The appearance of the energetically less favored short-range order has been ascribed to thermal effects as well as to the preparation conditions.

Calculations were performed at the Paderborn Center for Parallel Computing (PC²). The authors acknowledge the Deutsche Forschungsgesellschaft (D-A-CH project FWF I958 and GRK 1464) for the financial support,.

- ¹ J. V. Barth, G. Costantini, K. Kern, *Nature*, 2005, 437, 671.
- ² C. D. Dimitrakopoulos, P. R. L. Malenfant, *Adv. Mater.*, 2002, 14, 99.
- ³ G. Witte, C. Woll, *J. Mater. Res.*, 2004, 19, 1889.
- ⁴ S. R. Forrest, *Nature*, 2004, 428, 911.
- ⁵ S. Blankenburg, W.G. Schmidt, *Phys. Rev. Lett.*, 2007, 99, 196107.
- ⁶ A. K. Tripathi and J. Pflaum, *Appl. Phys. Lett.*, 2006, 89, 082103.
- ⁷ S. Sellner, A. Gerlach, F. Schreiber, M. Kelsch, N. Kasper, H. Dosch, S. Meyer, J. Pflaum, M. Fischer, and B. Gompf, *Adv. Mater.*, 2004, 16, 1750.
- ⁸ A. C. Dürr, F. Schreiber, M. Munch, N. Karl, B. Krause, V. Kruppa and H. Dosch, *Appl. Phys. Lett.*, 2002, 81, 2276.
- ⁹ X. N. Zhang, E. Barrena, D. G. de Oteyza, E. De Souza and H. Dosch, *J. Appl. Phys.*, 2008, 104, 104308.
- ¹⁰ S. Kowarik, A. Gerlach, S. Sellner, F. Schreiber, L. Cavalcanti and O. Kononov, *Phys. Rev. Lett.*, 2006, 96, 125504.
- ¹¹ N. Karl, *Synth. Met.*, 2003, 133, 649.
- ¹² M. B. Casu, I. Biswas, B.-E. Schuster, M. Nagel, P. Nagel, S. Schuppler, T. Chassé, *Appl. Phys. Lett.*, 2008, 93, 24103.
- ¹³ J. Wagner, M. Gruber, A. Hinderhofer, A. Wilke, B. Bröker, J. Frisch, P. Amsalem, A. Vollmer, A. Opitz, N. Koch, F. Schreiber, W. Brütting, *Adv. Funct. Mater.*, 2010, 20, 4295.
- ¹⁴ A. C. Dürr, F. Schreiber, K. A. Ritley, V. Kruppa, J. Krug, H. Dosch and B. Struth, *Phys. Rev. Lett.*, 2003, 90, 016104.
- ¹⁵ U. Heinemeyer, K. Broch, A. Hinderhofer, M. Kytka, R. Scholz, A. Gerlach, and F. Schreiber, *Phys. Rev. Lett.*, 2010, 104, 257401.
- ¹⁶ X. N. Zhang, E. Barrena, D. G. de Oteyza, H. Dosch, *Surf. Sci.*, 2007, 601, 2420–2425.
- ¹⁷ X. N. Zhang, D. G. de Oteyza, Y. Wakayama, H. Dosch, *Surf. Sci.*, 2009, 603, 3179–3183.
- ¹⁸ D. G. de Oteyza, E. Barrena, H. Dosch and Y. Wakayama, *Phys. Chem. Chem. Phys.*, 2009, 11, 8741–8744.
- ¹⁹ D. G. de Oteyza, J. M. García-Lastra, M. Corso, B. P. Doyle, L. Floreano, A. Morgante, Y. Wakayama, A. Rubio, J. Enrique Ortega, *Adv. Funct. Mater.* 2009, 19, 3567–3573.
- ²⁰ C. Bürker, N. Ferri, A. Tkatchenko, A. Gerlach, J. Niederhausen, T. Hosokai, S. Duhm, J. Zegenhagen, N. Koch and F. Schreiber, *Phys. Rev. B*, 2013, 87, 165443.
- ²¹ B. Schuler, W. Liu, A. Tkatchenko, N. Moll, G. Meyer, A. Mistry, D. Fox, L. Gross, *Phys. Rev. Lett.*, 2013, 111, 106103.
- ²² H. Huang, J.-T. Sun, Y. P. Feng, W. Chen, A. T. S. Wee, *Phys. Chem. Chem. Phys.*, 2011, 13, 20933–20938.
- ²³ D. G. de Oteyza, E. Barrena, H. Dosch, J. E. Ortega, Y. Wakayama, *Phys. Chem. Chem. Phys.*, 2011, 13, 4220–4223.
- ²⁴ E. Barrena, D. G. de Oteyza, H. Dosch and Y. Wakayama, *ChemPhysChem*, 2007, 8, 1915–1918.
- ²⁵ M. B. Casu, B. Schuster, I. Biswas, C. Raisch H. Marchetto, T. Schmidt and T. Chassé, *Adv. Mater.*, 2010, 22, 3740–3744.
- ²⁶ D. G. de Oteyza, E. Barrena, M. Ruiz-Osés, I. Silanes, B. P. Doyle, J. E. Ortega, A. Arnau, H. Dosch, Y. Wakayama, *J. Phys. Chem. C*, 2008, 112, 7168–7172.
- ²⁷ M. B. Casu, S.-A. Savu, B.-E. Schuster, I. Biswas, C. Raisch, H. Marchetto, Th. Schmidt and T. Chassé, *Chem. Commun.*, 2012, 48, 6957–6959.
- ²⁸ M. B. Casu, S.-A. Savu, P. Hoffmann, B.-E. Schuster, T. O. Mentese, M. A. Niño, A. Locatelli, T. Chassé, *CrystEngComm*, 2011, 13, 4139.
- ²⁹ A. C. Dürr, N. Koch, M. Kelsch, A. Rühm, J. Ghijsen, R. L. Johnson, J.-J. Pireaux, J. Schwartz, F. Schreiber, H. Dosch, and A. Kahn, *Phys. Rev. B*, 2003, 68, 115428.
- ³⁰ J. Tersoff and D. R. Hamann, *Phys. Rev. B*, 1985, 31, 805.
- ³¹ G. Kresse, J. Furthmüller, *Comput. Mater. Sci.* 1996, 6, 15–50.
- ³² J. P. Perdew, J. A. Chevary, S. H. Vosko, K. A. Jackson, M. R. Pederson, D. J. Singh, C. Fiolhais, *Phys. Rev. B*, 1992, 46, 6671–6687.
- ³³ G. Kresse, D. Joubert, *Phys. Rev. B*, 1999, 59, 1758–1775.
- ³⁴ F. Ortman, F. Bechstedt, and W G Schmidt, *Phys. Rev. B*, 2006, 73, 205101.
- ³⁵ E.R. McNellis, J. Meyer, and K. Reuter, *Phys. Rev. B*, 2009, 80, 205414-10.
- ³⁶ C. Thierfelder, M. Witte, S. Blankenburg, E. Rauls, and W.G. Schmidt, *Surf. Sci.* 2011, 605, 746–749.
- ³⁷ E. Rauls, T. Pertram, W.G. Schmidt, K. Wandelt, *Surf. Sci.* 2012, 606, 1120–1125.
- ³⁸ H. Aldahhak, E. Rauls, and W.G. Schmidt, *Surf. Sci.*, (In Press).
- ³⁹ H. Aldahhak, E. Rauls, and W.G. Schmidt, *Surf. Sci.*, (submitted).
- ⁴⁰ H. Aldahhak, W.G. Schmidt, and E. Rauls, *Surf. Sci.*, 2013, 617, 242–248.
- ⁴¹ Upon adsorption, structures of the adsorbate and the surface are distorted under the presence of one-another. If the energy of the adsorbate/surface in the current position with the current distorted geometry is given as E_{mol}^*/E_{sur}^* , the deformation energy E_{def} is then $E_{def} = (E_{sur}^* - E_{sur}) + (E_{mol}^* - E_{mol})$.
- ⁴² S. Wippermann and W.G. Schmidt, *Phys. Rev. Lett.*, 2010, 105, 126102.
- ⁴³ S. Blankenburg, E. Rauls and W.G. Schmidt, *Chem. Phys. Lett.*, 2010, 1, 3266.
- ⁴⁴ Q. Guo, A. Paulheim, M. Sokolowski, H. Aldahhak, E. Rauls, W. G. Schmidt, *The Journal of Physical Chemistry C*, 2014, 118, 29911–29918.